ENERGY AND EXERGY ANALYSES OF TWO-TEMPERATURE-LEVEL VAPOR COMPRESSION REFRIGERATION SYSTEMS FOR APPLICATIONS IN THE FOOD INDUSTRY
/
ANALIZA ENERGETICĂ ȘI EXERGETICĂ A SISTEMELOR FRIGORIFICE CU COMPRIMARE MECANICĂ DE VAPORI CU DOUĂ NIVELURI DE TEMPERATURĂ DESTINATE APLICAȚIILOR DIN INDUSTRIA ALIMENTARĂ

Daniel DIMA [1], George Daniel GHIȚĂ [*1], Mihai Florin BIZDADEA [*1], Horațiu POP [1], Valentin APOSTOL [1], Valentin CIOBANU [1], Cristian Marian SORICĂ [2*]

[1] National University of Science and Technology POLITEHNICA Bucharest / Romania;
[2] National Institute of Research – Development for Machines and Installations Designed to Agriculture and Food Industry - INMA Bucharest, Romania

Ghiță George Daniel; E-mail: george_daniel.ghita@upb.ro
Bizdadea Mihai Florin; E-mail: mihai.bizdadea@upb.ro
DOI: https://doi.org/10.35633/inmateh-79-107

Keywords: *exergy analysis, two-temperature-level, refrigeration and freezing system, throttling process, exergy destruction, coefficient of performance, low-GWP refrigerants.*

ABSTRACT
This study compares energy and exergy performance of two vapour-compression refrigeration systems designed to provide simultaneous refrigeration and freezing at two distinct temperature levels for food-industry applications. The simulation results indicated that R1234yf provided the best overall performance for both configurations. The exergy analysis showed that the throttling processes in the first configuration had the fastest increase in exergy destruction with the variation of ambient temperature. The structural improvement of the second configuration led to an increase in overall system performance, confirming the importance of refrigerant selection and structural optimisation of the refrigeration system. For R1234yf, the energy coefficient of performance increased from 2.69 to 2.97 at an ambient temperature of 35 °C and from 1.98 to 2.24 at 45 °C when configuration (b) was used instead of configuration (a).

REZUMAT
Acest studiu compară performanța energetică și exergetică a două sisteme frigorifice cu comprimare mecanică de vapori, proiectate pentru a asigura simultan refrigerarea și congelarea la două niveluri distincte de temperatura, pentru aplicații din industria alimentara. Rezultatele simulărilor au indicat faptul ca R1234yf a oferit cea mai bună performanță globală pentru ambele configurații. Analiza exergetică a arătat ca procesele de laminare din prima configurație au prezentat cea mai rapida creștere a distrugerii de exergie odată cu variația temperaturii ambiante. Îmbunătățirea structurala a celei de-a doua configurații a condus la creșterea performantei globale a sistemului, confirmând importanta selecției agentului frigorific si a optimizării structurale a sistemului frigorific.

INTRODUCTION
In agri-food applications, temperature requirements vary according to the specific characteristics of each product and its intended technological use. Some products must be stored under refrigeration conditions, whereas others require freezing conditions. Two-temperature-level refrigeration systems are used in food storage facilities, commercial units and cold-chain applications where different thermal conditions must be provided simultaneously. These systems can provide one temperature level for refrigeration and another for freezing, either within the same installation or through interconnected refrigeration configurations, such as cascade systems or other forms of thermal coupling.

Refrigeration and freezing are essential technologies for the preservation of agri-food products, as low temperatures reduce microbial activity, slow down enzymatic reactions and limit quality losses. Horticultural and food products have a high water content and deteriorate rapidly during storage, transport and distribution. For this reason, the use of artificial cold through refrigeration or freezing represents one of the most effective methods for preserving perishable products (*Sorică et al., 2023*).

For fresh fruit, storage in climate-controlled rooms contributes to maintaining appearance, firmness and nutritional characteristics during storage (*Hou et al., 2023*). Low-temperature storage is also important for grain preservation, where accurate temperature control can limit biological deterioration and maintain storage conditions. *Han and Leng (2026)* investigated an intelligent control strategy for low-temperature grain storage, demonstrating the potential of precise thermal regulation for agricultural product preservation. For food products of animal origin, refrigeration, partial freezing, and controlled-atmosphere packaging have been investigated as solutions for maintaining quality and extending storage life (*Hou et al., 2024*). For fish and other frozen products, freezing time is a key parameter because it influences product structure, water loss and final quality. *Ren et al. (2026)* experimentally investigated an industrial horizontal plate freezer integrated into a CO_2 refrigeration system. Decreasing the mean evaporating temperature from (-36.1°C) to (-48.6°C) reduced the average freezing time by 35.3%. However, the authors showed that lowering the evaporating temperature reduced the coefficient of performance (COP), while the specific energy consumption remained nearly unchanged because the shorter freezing time partly compensated for the lower performance of the refrigeration cycle.

Another major issue in the agri-food industry is the energy consumption of refrigeration systems. The food chain has a high energy demand, and the choice of refrigeration technology can significantly influence operating costs and environmental impact. *Ferretto et al. (2025)* analysed refrigeration systems for commercial food refrigeration and showed that the refrigerant and system configuration should be selected according to the application and climatic conditions. At the same time, the performance of refrigeration systems is sensitive to ambient temperature, particularly in commercial applications where operation is continuous and the refrigeration load varies over time (*Ferretto et al., 2025; Tsimpoukis et al., 2024*).

The selection of the refrigerant is influenced by regulations aimed at reducing fluorinated greenhouse gas emissions. Refrigerants with a high global warming potential are being progressively restricted, while low-GWP working fluids are increasingly used in commercial and industrial refrigeration systems. *Regulation (EU) 2024/573* establishes the current framework for fluorinated greenhouse gases and replaces *Regulations (EU) No 517/2014*. In this context, R448A, R449A, R454C and R1234yf were considered as working fluids in relation to the requirements established by the aforementioned EU Regulation. R449A and R454C have been investigated in commercial refrigeration systems and food applications, whereas R448A is used in supermarket refrigeration installations (*Ferretto et al., 2025; Giménez-Prades et al., 2024; Tsimpoukis et al., 2024*). R1234yf has also been analysed as a low-GWP refrigerant in studies concerning the energy and exergy performance of vapour-compression refrigeration systems (*Aized et al., 2022*).

Energy analysis is used to assess the overall performance of refrigeration systems through the coefficient of performance. However, exergy analysis is used to evaluate individual processes, as it identifies exergy destruction in each component and highlights the main sources of irreversibility. *Altinkaynak (2021)* analysed R448A and R449A as alternatives to R404A and compared their coefficient of performance, exergy efficiency, and distribution of exergy destruction. *Aized et al. (2022)* applied energy and exergy analyses to several low-GWP refrigerants, including R1234yf. In industrial cold-storage applications, exergy analysis is used to identify components with high exergy destruction and to establish directions for the optimisation of refrigeration systems (*Aksoy and Çerçi, 2026)*. In the same context, the development of IoT systems for refrigeration installations has shown that real-time data acquisition, thermodynamic calculations and control functions can support the transition from passive monitoring to the intelligent operation of refrigeration systems (*Bizdadea et al., 2025*).

Recent studies have applied exergy analysis to evaluate and optimise refrigeration systems and other thermal systems at both component and overall system levels (*Aized et al., 2022; Mamut and Sciubba, 2025; Roy and Mandal, 2023*). In the present study, exergy analysis was used to investigate the individual thermodynamic processes occurring within each refrigeration system. The distribution of exergy destruction was analysed to identify the components and processes that limit the performance of the two configurations and account for the differences in their overall performance. Building on the previous study by Ciobanu et al. [6], which compared several two-temperature-level refrigeration configurations mainly from an energy-performance perspective, the present work focuses on two selected configurations and extends the analysis by including a detailed exergy assessment, the distribution of exergy destruction among the main processes, and the influence of ambient temperature. The aim of this paper is therefore to compare the energy and exergy performance of these two vapour-compression refrigeration systems for simultaneous refrigeration and freezing applications in the food industry, using R448A, R449A, R454C and R1234yf as working fluids.

MATERIALS AND METHODS

Selection of Working Fluids

The refrigerants were preliminarily selected based on the literature review, current European Union requirements, environmental characteristics, safety classification and thermodynamic properties. Particular attention was given to the saturation pressure at the freezing-chamber evaporation temperature. Table 1 summarises the relevant characteristics of the candidate fluids at (-29°C) (*ASHRAE-UNEP, 2024; Danfoss Group, 2024*).

R448A, R449A, R454C and R1234yf were retained for the comparative analysis. By contrast, R1233zd(E) and R1234ze(E) were excluded because their saturation pressures at (−29°C) were below atmospheric pressure, which would require sub-atmospheric operation on the low-pressure side under the considered operating conditions. Unlike the previous study by *Ciobanu et al. (2025)*, where compression was assumed to be adiabatic and reversible, both compressors in the present study were modelled as adiabatic devices with a constant isentropic efficiency of 0.80, thereby accounting for compressor irreversibility. This value was selected based on the 0.80-0.90 range reported by *Çengel et al. (2019)* for well-designed compressors and on the recent study by *Liu et al. (2026)*, in which compressor isentropic efficiencies between 0.65 and 0.85, including 0.80, were investigated for an R1234yf refrigeration system. Pressure losses in the refrigerant lines and heat exchangers were neglected. The intermediate pressure was defined as the saturation pressure corresponding to the evaporation temperature of the refrigeration chamber.

Table 1

Characteristics of the refrigerants considered in the study and saturation pressure at the freezing-chamber evaporation temperature

No.	Refrigerant	ODP	GWP	Safety class	Refrigerant type	Saturation pressure at −29 °C [bar]
1.	R448A	0	1387	A1	Zeotropic blend	1.68
2.	R449A	0	1397	A1	Zeotropic blend	1.68
3.	R454C	0	148	A2L	Zeotropic blend	1.50
4.	R1234yf	0	4	A2L	Pure fluid	1.03
5.	R1233zd(E)	0	4.5	A1	Pure fluid	0.11
6.	R1234ze(E)	0	7	A2L	Pure fluid	0.64

Description of the Refrigeration Systems

Two configurations of two-temperature-level vapour-compression refrigeration systems were analysed. Both configurations were designed to provide refrigeration and freezing simultaneously, under the same operating conditions. The main parameters used in the comparative energy and exergy analyses are presented in Table 2.

Table 2

Main operating parameters used in the analysis

No.	Parameter	Symbol	Value	UM
1.	Freezing-chamber temperature	t_f	-25	°C
2.	Refrigeration-chamber temperature	t_r	0	°C
3.	Ambient temperature, decision variable	t_0	35÷45	°C
4.	Minimum temperature difference in the heat exchangers	ΔT_{HE}	5	K
5.	Cooling capacity corresponding to the refrigeration load	$\dot{Q}_{\mathrm{ev},r}$	1	kW
6.	Cooling capacity corresponding to the freezing load	$\dot{Q}_{\mathrm{ev},f}$	0.421	kW

The schematic diagram of refrigeration system (a) and the corresponding thermodynamic cycle are shown in Fig. 1. Refrigeration system (a) comprises a refrigeration evaporator (Ev_r), a freezing evaporator (Ev_f), three throttling valves (Tv_1, Tv_2 and Tv_3), a high-stage compressor (C_{p1}), a low-stage compressor (C_{p2}), a condenser (Cd), and a liquid separator (Sl).

The refrigeration evaporator (Ev_r) provides the refrigeration load, whereas the freezing evaporator (Ev_f) provides the freezing load. The refrigerant from vapour leaving the freezing evaporator (Evf) is compressed by the low-stage compressor (C_{p2}), while the high-stage compressor (C_{p1}) raises the pressure of the combined refrigerant flow to the condensing pressure. Expansion valve (Tv_3) is installed upstream of the liquid separator (*Sl*) and reduces the pressure of part of the liquid refrigerant leaving the condenser to the intermediate-pressure level. The liquid separator connects the refrigerant branches operating at the two pressure levels.

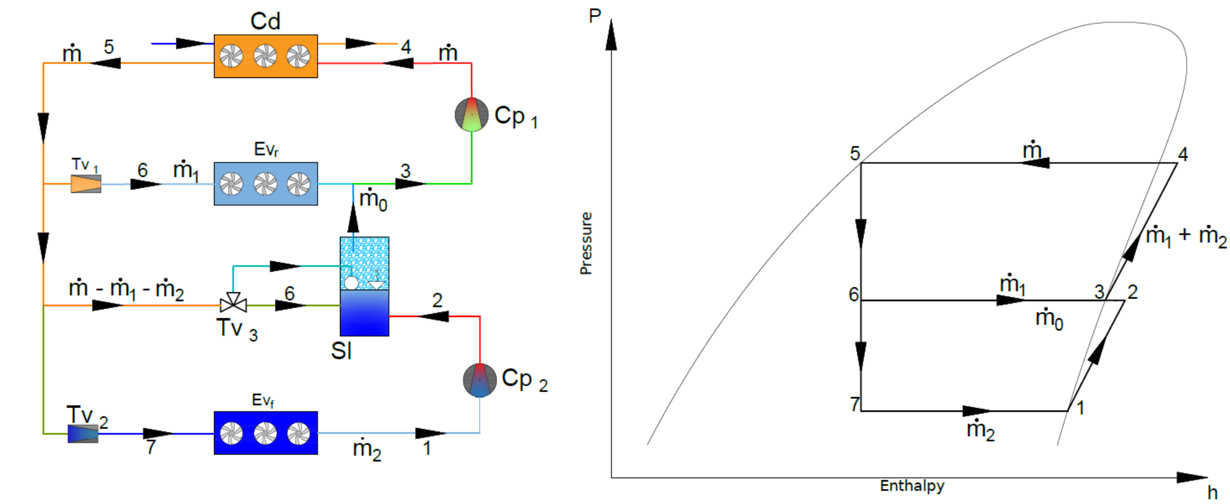

Fig. 1 – Two-temperature-level refrigeration and freezing system (a): schematic diagram (left) and corresponding thermodynamic cycle in the p-h diagram (right)

C_{p1} – high-stage compressor; C_{p2} – low-stage compressor; Cd – condenser; Ev_r – refrigeration evaporator; Ev_f – freezing evaporator; Tv_1, Tv_2 and Tv_3 – throttling valves; Sl –liquid separator; $\dot{m},\dot{m}_0,\dot{m}_1$ and $\dot{m}_2$– refrigerant mass flow rates; 1–7 – thermodynamic state points.; p – pressure; h – specific enthalpy. Source: adapted from Ciobanu et al. (2025).

Refrigeration system (b) includes the same main components as refrigeration system (a). However, the connection of the liquid separator (*Sl*) and the arrangement of the freezing branch differ from those of system (a). In system (b), the refrigerant discharged by the low-stage compressor (C_{p2}) enters the liquid separator, together with the two-phase refrigerant stream produced by throttling through expansion valve (Tv_3). Intercooling and phase separation occur in (*Sl*) at the intermediate-pressure level. The vapour leaving the liquid separator mixes with the refrigerant flow from the refrigeration evaporator (Ev_r) before entering the high-stage compressor (C_{p1}). The liquid phase leaving the separator is expanded through (Tv_2) and subsequently supplied to the freezing evaporator (Ev_f). The schematic diagram of refrigeration system (b) and the corresponding thermodynamic cycle are presented in Fig. 2.

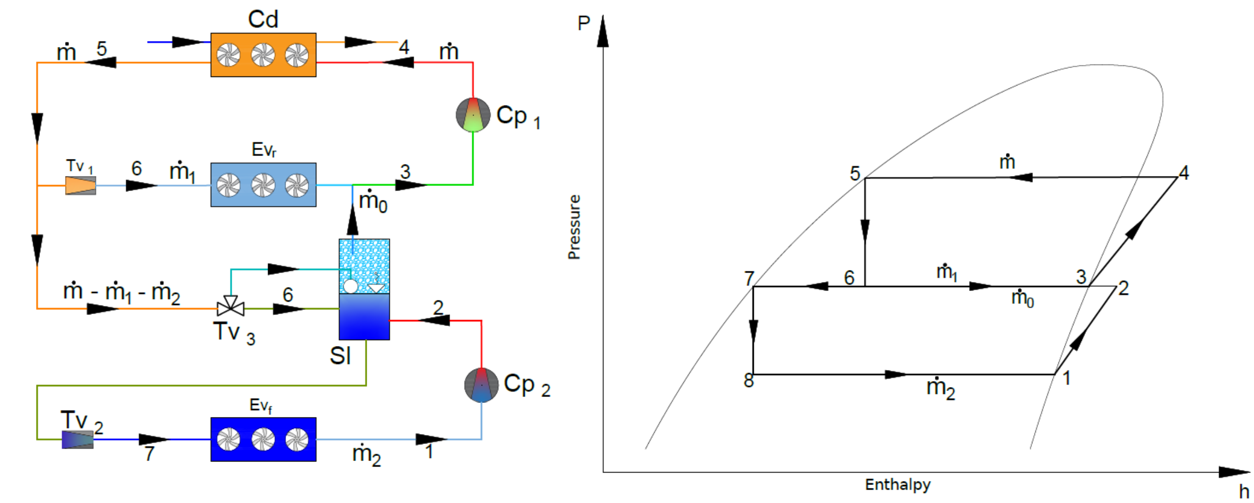

Fig. 2 – Two-temperature-level refrigeration and freezing system (b): schematic diagram (left) and corresponding thermodynamic cycle in the p-h diagram (right)

Cd – condenser; C_{p1} – high-stage compressor; C_{p2} – low-stage compressor; Ev_r – refrigeration evaporator; Ev_f – freezing evaporator; Tv_1, Tv_2 and Tv_3 – throttling valves; Sl –liquid separator; $\dot{m},\dot{m}_0,\dot{m}_1$ and $\dot{m}_2$– refrigerant mass flow rates; 1–8 – thermodynamic state points.; p – pressure; h – specific enthalpy.
Source: adapted from Ciobanu et al. (2025).

Mathematical Model of Refrigeration System (a)

After establishing the refrigeration loads and the main operating parameters of the two systems according to the data presented in Table 2, the mathematical models were developed. Energy balances were used to evaluate the overall performance of the systems, whereas exergy analysis was applied to identify the processes associated with the highest exergy destruction. The mathematical models were implemented using Engineering Equation Solver (EES) software (F-Chart Software, n.d.).

Refrigeration system (a), presented in Fig. 1, provides the required cooling loads at two temperature levels, corresponding to refrigeration and freezing applications. Based on the overall energy balance derived from the first law of thermodynamics, the following relationship can be written *(Russell and Adebiyi, 1993)*:

$$\dot{Q}^a_{ev_f} + \dot{Q}^a_{ev_r} + \dot{W}^a_{cp_1} + \dot{W}^a_{cp_2} = \dot{Q}^a_{cd} \tag{1}$$

where: $\dot{Q}^a_{ev_f} and \dot{Q}^a_{ev_r}$ are the cooling capacities corresponding to the freezing and refrigeration loads, respectively, [kW]; $\dot{W}^a_{cp_1} and\ \dot{W}^a_{cp_2}$ are the power inputs of the high-stage and low-stage compressors, respectively, [kW]; $\dot{Q}^a_{cd}$ is the heat transfer rate from the refrigerant to the surroundings in the condenser, [kW]; and superscript a denotes refrigeration system (a).

The cooling capacity corresponding to the freezing load is calculated as:

$$\dot{Q}^a_{ev_f} = \dot{m}_2(h_1 - h_7) \tag{2}$$

The cooling capacity corresponding to the refrigeration load is calculated as:

$$\dot{Q}^a_{ev_r} = \dot{m}_1(h_3 - h_6) \tag{3}$$

where: $\dot{m}_1 and\ \dot{m}_2$ are the refrigerant mass flow rates through the refrigeration and freezing evaporators, respectively, [kg/s], while $h_1, h_3, h_6\ and\ h_7$ are the specific enthalpies at the corresponding thermodynamic state points, [kJ/kg].

The power input of the high-stage compressor is:

$$\dot{W}^a_{cp_1} = \dot{m}(h_4 - h_3) \tag{4}$$

The power input of the low-stage compressor is:

$$\dot{W}^a_{cp_2} = \dot{m}_2(h_2 - h_1) \tag{5}$$

where: $\dot{m}$ is the total refrigerant mass flow rate through the high-stage compressor, [kg/s], and $h_1, h_2, h_3\ and\ h_4$ are the specific enthalpies at the corresponding compressor inlet and outlet state points, [kJ/kg].

The heat transfer rate rejected by the condenser is:

$$\dot{Q}^a_{cd} = \dot{m}(h_5 - h_4) \tag{6}$$

where: h_5 is the specific enthalpy at the condenser outlet, [kJ/kg].

The overall energy coefficient of performance of refrigeration system (a) is defined as:

$$COP^a_{en} = \frac{\dot{Q}^a_{ev_f} + \dot{Q}^a_{ev_r}}{\dot{W}^a_{cp_1} + \dot{W}^a_{cp_2}} \tag{7}$$

Exergy analysis was applied to evaluate the thermodynamic performance of the individual processes. For the complete refrigeration system operating under steady-state conditions, the general exergy balance is written as follows (*Radcenco, 1977*).

$$\sum \dot{Ex}^{T_i}_{Q_i} + \sum \dot{I}_i = \sum \dot{W}_i \tag{8}$$

where: $\dot{Ex}^{T_i}_{Q_i}$ is the exergy transfer rate associated with heat transfer at temperature T_i, [kW]; $\dot{W}_i$ is the power transfer rate, [kW]; $\dot{I}_i$ is the exergy destruction rate of component or process i, [kW]; and T_i is the absolute temperature at which heat transfer occurs, [K].

Applying Equation (8) to refrigeration system (a) gives:

$$\dot{Ex}^{T_{7-1}}_{Q^a_{ev_f}} + \dot{Ex}^{T_{6-3}}_{Q^a_{ev_r}} + \dot{I}^a_{cp_1} + \dot{I}^a_{cp_2} + \dot{I}^a_{tv_1} + \dot{I}^a_{tv_2} + \dot{I}^a_{tv_3} + \dot{I}^a_{ls} + \dot{I}^a_{cd} = \dot{W}^a_{cp_1} + \dot{W}^a_{cp_2} \tag{9}$$

where: $\dot{Ex}^{T_{7-1}}_{Q^a_{ev_f}}$ and $\dot{Ex}^{T_{6-3}}_{Q^a_{ev_r}}$ are the exergy transfer rates associated with the heat absorbed in the freezing and refrigeration evaporators, respectively, [kW]; $\dot{I}^a_{cp_1}$ and $\dot{I}^a_{cp_2}$ are the exergy destruction rates in the high-stage and low-stage compressors, respectively, [kW]; $\dot{I}^a_{tv_1}, \dot{I}^a_{tv_2}$ and $\dot{I}^a_{tv_3}$ are the exergy destruction rates associated with the throttling processes, [kW]; $\dot{I}^a_{ls}$ is the exergy destruction rate in the liquid separator, [kW]; and $\dot{I}^a_{cd}$ is the exergy destruction rate in the condenser, [kW].

After identifying the exergy fuel and exergy product of the system, *Equation (9)* can be expressed in fuel-product form as follows:

$$\dot{W}^a_{cp_1} + \dot{W}^a_{cp_2} = \dot{Ex}^{T_f}_{Q^a_{ev_f}} + \dot{Ex}^{T_r}_{Q^a_{ev_r}} + \dot{I}^a_{cp_1} + \dot{I}^a_{cp_2} + \dot{I}^a_{ev_f} + \dot{I}^a_{ev_r} + \dot{I}^a_{tv_1} + \dot{I}^a_{tv_2} + \dot{I}^a_{tv_3} + \dot{I}^a_{ls} + \dot{I}^a_{cd} \tag{10}$$

The exergy coefficient of performance of refrigeration system (a) is calculated as:

$$\eta^a_{ex} = \frac{\dot{Ex}^{T_f}_{Q^a_{ev_f}} + \dot{Ex}^{T_r}_{Q^a_{ev_r}}}{\dot{W}^a_{cp_1} + \dot{W}^a_{cp_2}} \cdot 100 \tag{11}$$

where: η^a_{ex} is the exergy coefficient of performance of refrigeration system (a), [%].

Mathematical Model of Refrigeration System (b)

The configuration shown in Fig. 2 represents refrigeration system (b), which is also designed to meet refrigeration and freezing loads at two distinct temperature levels. The corresponding energy and exergy relations are developed below for this system arrangement.

The energy balance derived from the first law of thermodynamics and applied to refrigeration system (b) is written as follows:

$$\dot{Q}^b_{ev_f} + \dot{Q}^b_{ev_r} + \dot{W}^b_{cp_1} + \dot{W}^b_{cp_2} = \dot{Q}^b_{cd} \tag{12}$$

where: superscript b denotes refrigeration system (b), while the remaining terms have the same meanings and units as those defined for *Equation (1)*.

The overall energy coefficient of performance of refrigeration system (b) is calculated:

$$\mathrm{COP}^b_{en} = \frac{\dot{Q}^b_{ev_f} + \dot{Q}^b_{ev_r}}{\dot{W}^b_{cp_1} + \dot{W}^b_{cp_2}} \tag{13}$$

where: COP^b_{en} is the overall energy coefficient of performance of refrigeration system (b), [–].

The exergy balance of refrigeration system (b), expressed in terms of exergy fuel, exergy product and exergy destruction, is written as:

$$\dot{W}^b_{cp_1} + \dot{W}^b_{cp_2} = \dot{Ex}^{T_f}_{Q^b_{ev_f}} + \dot{Ex}^{T_r}_{Q^b_{ev_r}} + \dot{I}^b_{cp_1} + \dot{I}^b_{cp_2} + \dot{I}^b_{ev_f} + \dot{I}^b_{ev_r} + \dot{I}^b_{tv_1} + \dot{I}^b_{tv_2} + \dot{I}^b_{tv_3} + \dot{I}^b_{ls} + \dot{I}^b_{cd} \tag{14}$$

where: the exergy-transfer and exergy-destruction terms have the same meanings and units as those defined for refrigeration system (a), while superscript b indicates that the terms refer to refrigeration system (b).

The exergy efficiency of refrigeration system (b) is calculated as:

$$\eta^b_{ex} = \frac{\dot{Ex}^{T_f}_{Q^b_{ev_f}} + \dot{Ex}^{T_r}_{Q^b_{ev_r}}}{\dot{W}^b_{cp_1} + \dot{W}^b_{cp_2}} \cdot 100 \tag{15}$$

where: η^b_{ex} is the exergy efficiency of refrigeration system (b), [%].

The exergy transfer rate associated with heat transfer is calculated as:

$$\dot{Ex}^{T_i}_{Q_i} = \dot{Q}_i \left(\frac{T_0}{T_i} - 1\right) \tag{16}$$

where: $\dot{Ex}^{T_i}_{Q_i}$ is the exergy transfer rate associated with heat transfer in process i, [kW]; $\dot{Q}_i$ is the corresponding heat transfer rate, [kW]; T_0 is the ambient reference temperature, [K]; and T_i is the absolute temperature at which heat transfer occurs, [K].

The exergy destruction rate of each process is calculated as:

$$\dot{I}_i = T_0 \dot{S}_{gen_i} \tag{17}$$

where: $\dot{I}_i$ is the exergy destruction rate of process i, [kW], and $\dot{S}_{gen_i}$ is the entropy generation rate associated with the process, [kW/K].

The relative exergy destruction associated with each process, expressed with respect to the total compressor power input, is calculated as:

$$\psi_i = \frac{\dot{I}_i}{\sum_i \dot{W}_i} \cdot 100 \tag{18}$$

where: ψ_i is the relative exergy associated with each process i, [%], and $\sum_i \dot{W}_i$ is the total compressor power input, [kW].

RESULTS

To identify the working fluid providing the highest overall performance for the two investigated refrigeration systems, the overall energy and exergy coefficients of performance were evaluated for R448A, R449A, R454C and R1234yf. The ambient temperature, t_0, was varied from 35 *°C* to 45 *°C* and was used as the independent variable in the sensitivity analysis.

For refrigeration system (a), the overall energy coefficient of performance decreased with increasing ambient temperature for all the investigated refrigerants, as shown in Fig.3. R1234yf provided the highest values over the entire temperature range, followed by R448A, R449A and R454C. The energy coefficient of performance obtained with R1234yf decreased from approximately 2.69 at 35*°C* to approximately 1.98 at 45*°C*.

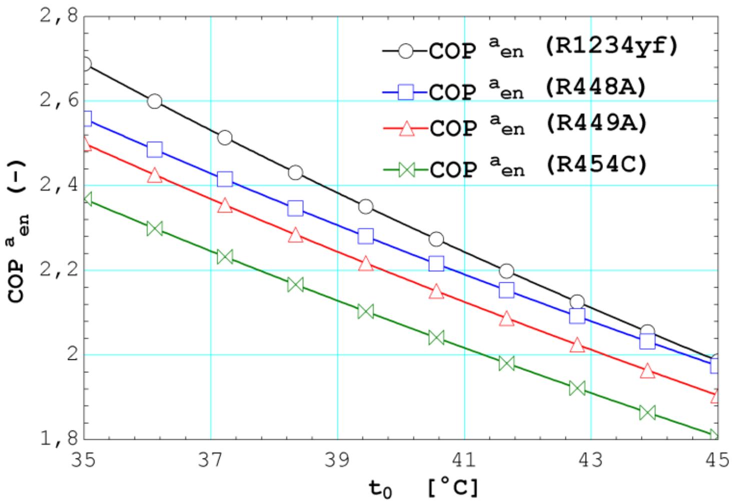

Fig. 3 - Variation of the overall energy coefficient of performance of refrigeration system (a) with ambient temperature for the investigated refrigerants

A similar tendency was obtained for the exergy coefficient of performance of refrigeration system (a), as presented in Fig. 4. The values decreased as the ambient temperature increased, while the ranking of the refrigerants remained unchanged. R1234yf provided the highest exergy coefficient of performance, which decreased from approximately 43.6% to 39.7% over the investigated temperature range. R454C showed the lowest values.

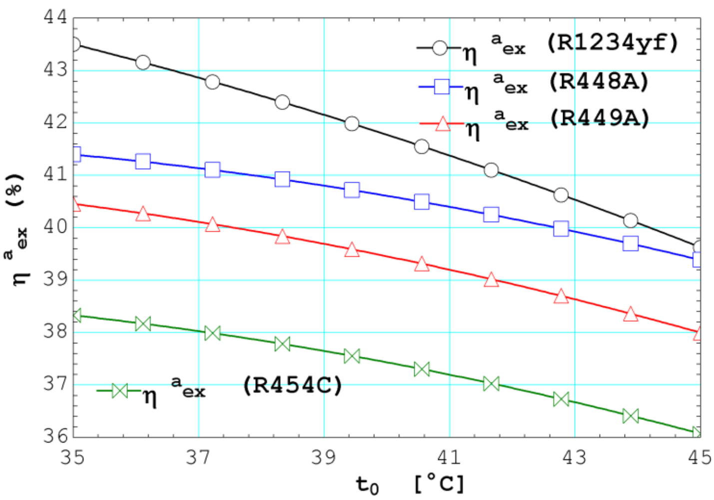

Fig. 4 - Variation of the exergy coefficient of performance of refrigeration system (a) with ambient temperature for the investigated refrigerants

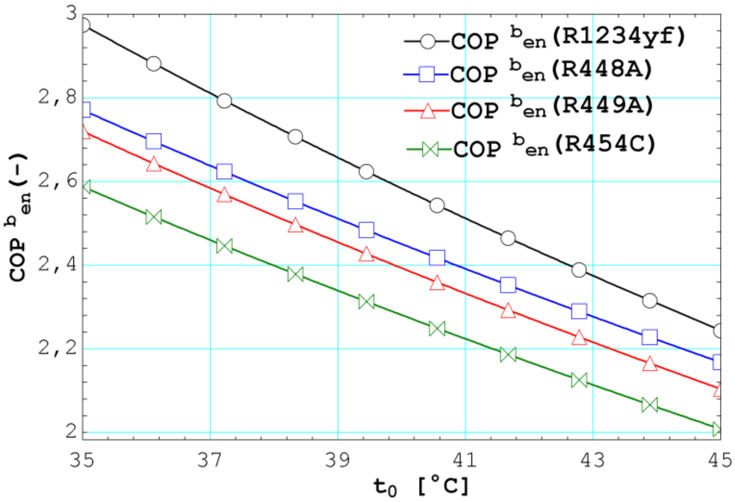

Fig. 5 - Variation of the overall energy coefficient of performance of refrigeration system (b) with ambient temperature for the investigated refrigerants

The results obtained for refrigeration system (b) are presented in Figs. 5 and 6. The overall energy coefficient of performance decreased with increasing ambient temperature for all four refrigerants. R1234yf again provided the highest values, followed by R448A, R449A and R454C. For R1234yf, the energy coefficient of performance decreased from approximately 2.97 at 35 *°C* to approximately 2.24 at 45 *°C*.

The exergy coefficient of performance of refrigeration system (b) followed the same decreasing tendency, as shown in Fig. 6. R1234yf provided the highest values, ranging from approximately 48.0% at 35 *°C* to approximately 44.7% at 45 *°C*. R454C presented the lowest exergy performance throughout the investigated range.

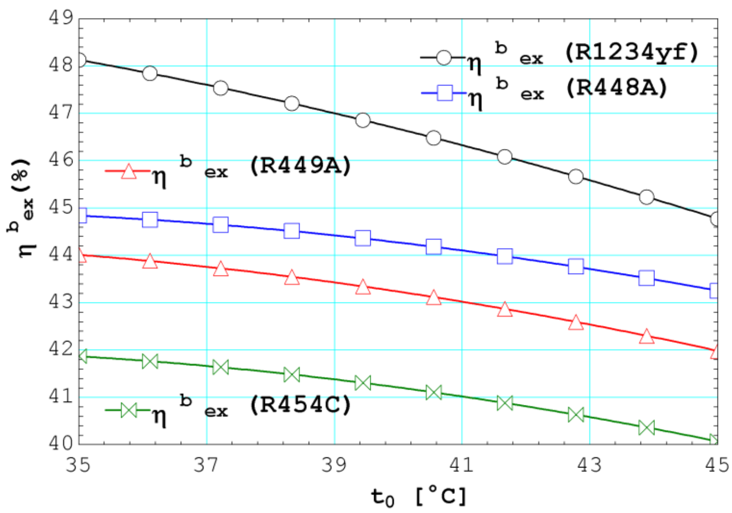

Fig. 6 - Variation of the exergy coefficient of performance of refrigeration system (b) with ambient temperature for the investigated refrigerants

The comparison of the results presented in Figs. 3–6 showed that refrigeration system (b) achieved higher energy and exergy performance than refrigeration system (a) under the same operating conditions. The influence of the system configuration was observed for all the investigated refrigerants. Based on the overall results, R1234yf was selected for the component-level exergy analysis of the two refrigeration systems.

The relative exergy destruction associated with the individual processes of refrigeration system (a) is presented in Fig. 7. The relative exergy destruction associated with the first and second throttling processes increased considerably with ambient temperature. The contribution of the high-stage compressor remained almost constant, whereas the relative contributions of the condenser, low-stage compressor and evaporators generally decreased over the investigated temperature range.

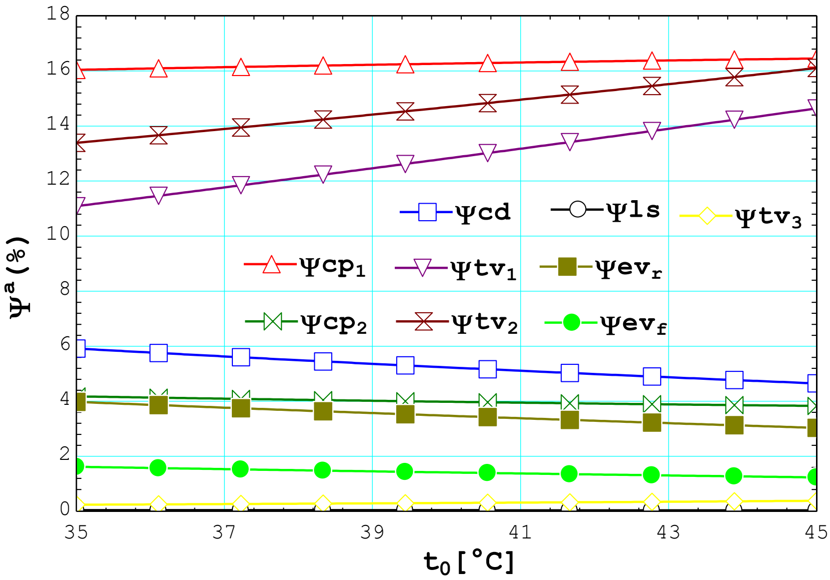

Fig. 7 - Relative exergy destruction associated with the individual processes of refrigeration system (a) using R1234yf

ψ^{a}– relative exergy destruction associated with system a

For refrigeration system (b), the distribution of relative exergy destruction is shown in Fig. 8. The contribution of the first throttling process increased with ambient temperature, while the third throttling process also showed an increasing tendency. The relative exergy destruction of the second throttling process remained comparatively low. The high-stage compressor represented one of the largest individual contributions, but its variation with ambient temperature is limited.

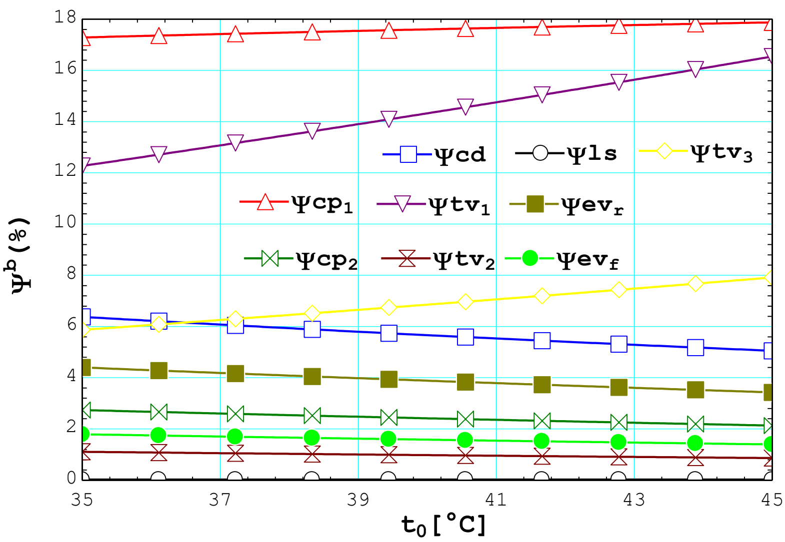

Fig. 8 - Relative exergy destruction associated with the individual processes of refrigeration system (b) using R1234yf

ψ^{b}– relative exergy destruction associated with system b

The total relative exergy destruction associated with the throttling processes of the two refrigeration systems is compared in Fig. 9. In both configurations, the total value increased with ambient temperature and followed a similar tendency. However, refrigeration system (b) maintained lower values throughout the investigated temperature range. For refrigeration system (a), the total relative exergy destruction of the throttling processes increased from approximately 24.6 % at 35 °*C* to approximately 31.1 % at 45°*C*. For refrigeration system (b), the corresponding values increased from approximately 19.1 % to approximately 25.2%.

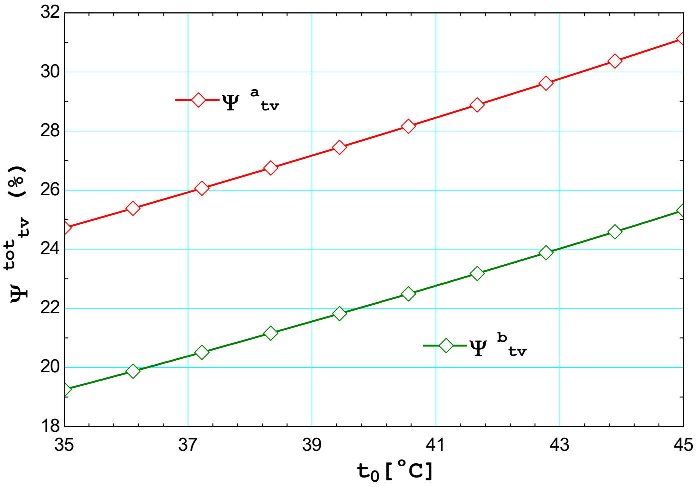

Fig. 9 - Total relative exergy destruction associated with the throttling processes of refrigeration systems (a) and (b) using R1234yf

ψ_{tv}^{tot} – total relative exergy destruction associated with the throttling processes; superscripts a and b denote refrigeration systems (a) and (b), respectively.

The comparison of Figs. 3–6 confirms the superior performance of refrigeration system (b) under the same operating conditions. For R1234yf, the COP of system (b) was approximately 10.4% higher than that of system (a) at 35 °C and 13.1% higher at 45 °C, while the corresponding improvements in exergy efficiency were approximately 10.1% and 12.6%, respectively. This performance advantage is consistent with the lower irreversibilities associated with the throttling processes in configuration (b), for which the total relative exergy destruction remained below that of configuration (a) over the entire investigated temperature range. These results indicate that the modified flow arrangement and intermediate-pressure separation in system (b) provide a thermodynamically more favourable distribution of irreversibilities.

CONCLUSIONS

An energy and exergy analysis was carried out for two refrigeration system configurations capable of simultaneously providing the temperature levels required for refrigeration and freezing. Their performances were evaluated using R448A, R449A, R454C and R1234yf under different ambient-temperature conditions.

The comparative analysis showed that the working fluid had a significant influence on the overall energy and exergy performance of both systems. Among the investigated refrigerants, R1234yf provided the highest energy and exergy coefficients of performance over the entire ambient-temperature range, while both indicators decreased as ambient temperature increased.

Although refrigeration systems (a) and (b) contained the same main components, their different structural arrangements led to different overall performances. Under the same operating conditions, system (b) provided higher energy and exergy coefficients of performance than system (a).

The process-level exergy analysis showed that the relative exergy destruction associated with the throttling processes presented the greatest sensitivity to ambient temperature. The staged throttling arrangement adopted in refrigeration system (b) reduced the total relative exergy destruction associated with these processes throughout the investigated temperature range. This reduction explained the improved overall performance of system (b).

Therefore, refrigerant selection and system configuration should be considered jointly when designing and optimising two-temperature-level refrigeration systems. Exergy analysis proved useful for identifying the main sources of irreversibility and supporting the development of more efficient systems for simultaneous refrigeration and freezing.

As a final conclusion, out of the two configurations investigated in the present paper, configuration (b) is the one recommended to be used in the food industry where both freezing and refrigeration are needed. Among the two configurations investigated, configuration (b) is recommended for food-industry applications requiring simultaneous refrigeration and freezing under the operating conditions and cooling capacities considered in this study. Further analysis is required before extending this conclusion to significantly larger-capacity refrigeration systems.

REFERENCES

[1] Aized T., Rashid M., Riaz F., Hamza A., Nabi H.Z., Sultan M., Ashraf W.M., Krzywanski J., (2022), Energy and exergy analysis of vapor compression refrigeration system with low-GWP refrigerants, *Energies*, vol. 15, no. 19, article 7246. DOI: https://doi.org/10.3390/en15197246

[2] Aksoy A.B., Çerçi Y., (2026), Energy–exergy–exergoeconomic evaluation of a two-stage ammonia refrigeration cycle under industrial operating conditions, *Applied Sciences*, vol. 16, no. 3, article 1163. DOI: https://doi.org/10.3390/app16031163

[3] Altinkaynak M., (2021), Exergetic performance analysis of low GWP alternative refrigerants for R404A in a refrigeration system, *International Journal of Low-Carbon Technologies*, vol. 16, no. 3, pp. 842–850. DOI: https://doi.org/10.1093/ijlct/ctaa104

[4] Bizdadea M.F., Ghiță G.D., Apostol V.G., Pop H.L., Grămescu B., (2025), Modular Internet of Things system for monitoring, control and alerting in refrigeration systems using ESP32 and Raspberry Pi 4, *EAI Endorsed Transactions on Digital Transformation of Industrial Processes*, vol. 1, no. 3. DOI: https://doi.org/10.4108/dtip.9792

[5] Çengel Y.A., Boles M.A., Kanoğlu M., (2019), *Thermodynamics: An Engineering Approach, 9th edition*, McGraw-Hill Education, New York, NY/USA. ISBN 978-1-259-82267-4.

[6] Ciobanu V., Apostol V., Pop H., Ioniță C., Dima D., (2025), Comparative performance analysis of commercial refrigeration systems with two temperature levels considering different refrigerants, *International Conference on Thermal Engineering – ICTEA*, vol. 1, no. 1.

[7] F-Chart Software, (n.d.), Engineering Equation Solver (EES). Available at: *https://fchartsoftware.com/ees/* (accessed on 20 July 2026)

[8] Ferretto W., Molinaroli L., Codella F., (2025), Performance assessment of R-454C, R-449A, and R-744 in food retail refrigeration systems, *Energies*, vol. 18, no. 3, article 667. DOI: https://doi.org/10.3390/en18030667

[9] Giménez-Prades P., Navarro-Esbrí J., Udroiu C.-M., Mota-Babiloni A., (2024), Influence of subcooling in R-449A supermarket refrigeration system and screening of refrigerant mixtures for its energetic and environmental improvement, *Applied Thermal Engineering*, vol. 236, article 121787. DOI: https://doi.org/10.1016/j.applthermaleng.2023.121787

[10] Han F., Leng Z., (2026), Multimodal scenario control method for low-temperature grain storage based on the AdaBelief algorithm (基于 AdaBelief 算法的低温粮食储存多模态场景控制方法), *INMATEH – Agricultural Engineering*, vol. 78, no. 1, pp. 192–202, Bucharest/Romania. DOI: https://doi.org/10.35633/inmateh-78-15

[11] Hou H., Cui S., Li D., Li Z., Chen Y., (2023), Effect of low-voltage electrostatic-field (LVEF) assisting refrigeration on preservation quality of strawberry (低压静电场辅助冷藏对草莓贮藏品质的影响), *INMATEH – Agricultural Engineering*, vol. 71, no. 3, pp. 657–666, Bucharest/Romania. DOI: https://doi.org/10.35633/inmateh-71-57

[12] Hou H., Li D., Zhang S., Niu W., Cui Q., Chen Y., (2024), Impact of partial freezing with modified atmosphere packaging on pork's quality (气调微冻对猪肉品质的影响), *INMATEH – Agricultural Engineering*, vol. 74, no. 3, pp. 127–136, Bucharest/Romania. DOI: https://doi.org/10.35633/inmateh-74-11

[13] Liu Y., Xie Y., Wang Z., Yang Z., Yang L., Dou B., (2026), Experimental research and simulation optimization of compression-type R1234yf hydrate cool storage system, *International Journal of Refrigeration*, vol. 185, pp. 336–348. DOI: https://doi.org/10.1016/j.ijrefrig.2026.02.028

[14] Mamut E., Sciubba E., (2025), Multi-scale extended exergy analysis of the "system Romania": A tool for monitoring the UN-2030 SDGs, *Energy*, vol. 314, article 134055. DOI: https://doi.org/10.1016/j.energy.2024.134055

[15] Pon Pavithiran C.K., Sakthivadivel D., Agarwal A., Agarwal A., (2025), Experimental investigation and thermo-enviro-economic analysis of a novel biomass driven dual-bed vapor adsorption refrigeration system for a cold storage room and bulk milk chiller for rural applications, *Thermal Science and Engineering Progress*, vol. 59, article 103327. DOI: https://doi.org/10.1016/j.tsep.2025.103327

[16] Radcenco V., (1977), *Optimization Criteria for Irreversible Thermal Processes (Criterii de optimizare a proceselor termice (ireversibile))*, Technical Publishing House (Editura Tehnică), Bucharest/Romania. (in Romanian)

[17] Ren S., Hadamitzky P., Hafner A., Widell K.N., (2026), Experimental analysis of freezing times for fish and dummy loads in a horizontal CO_2 plate freezer at −50 °C evaporation temperature, *International Journal of Refrigeration*, vol. 184, pp. 14–29. DOI: https://doi.org/10.1016/j.ijrefrig.2026.01.017

[18] Roy R., Mandal B.K., (2023), Energy, exergy and economic optimization of a two-stage refrigeration system using low-GWP alternative refrigerants for high-temperature lift applications, *Journal of the Brazilian Society of Mechanical Sciences and Engineering*, vol. 45, article 403. DOI: https://doi.org/10.1007/s40430-023-04320-9

[19] Russell L.D., Adebiyi G.A., (1993), *Classical Thermodynamics*, Oxford University Press, New York, NY/USA.

[20] Sorică C.M., Vlăduț N.-V., Grigore A.I., Cristea M., Sorică E., Oprescu R.M., Ionescu A., Vlăduțoiu L.C., Dumitrescu L., (2023), Cryogenic freezing of some berry species using an experimental model of multi-functional quick-freezing equipment (Congelarea criogenică a unor specii de fructe de pădure utilizând un model experimental de echipament multifuncțional de congelare rapidă), *INMATEH – Agricultural Engineering*, vol. 71, no. 3, pp. 451–458, Bucharest/Romania. DOI: https://doi.org/10.35633/inmateh-71-39

[21] Tsimpoukis D., Syngounas E., Bellos E., Koukou M., Tzivanidis C., Anagnostatos S., Vrachopoulos M.G., (2024), Data-driven energy efficiency comparison between operating R744 and R448A supermarket refrigeration systems based on hybrid experimental-simulation analysis, *Thermal Science and Engineering Progress*, vol. 53, article 102776. DOI: https://doi.org/10.1016/j.tsep.2024.102776

[22] *** ASHRAE–UNEP, (2026), Update on New Refrigerants Designations and Safety Classifications, Factsheet 1, *American Society of Heating, Refrigerating and Air-Conditioning Engineers and United Nations Environment Programme*. Available at: https://www.ashrae.org/file%20library/professional%20development/ashrae-unep/unep---ashrae-factsheet--english.pdf (accessed on 20 July 2026)

[23] *** Danfoss Group, (n.d.), *Refrigerants with low GWP*. Available at: https://www.danfoss.com/en/about-danfoss/our-businesses/cooling/refrigerants-and-energy-efficiency/refrigerants-for-lowering-the-gwp/ (accessed on 20 July 2026)

[24] *** European Union, (2024), Regulation (EU) 2024/573 of the European Parliament and of the Council of 7 February 2024 on fluorinated greenhouse gases, amending Directive (EU) 2019/1937 and repealing Regulation (EU) No 517/2014, *Official Journal of the European Union*, L 2024/573, 20 February 2024. Available at: https://eur-lex.europa.eu/eli/reg/2024/573/oj/eng